Optik 126 (2015) 3283–3287

Contents lists available at ScienceDirect

Optik

journal homepage: www.elsevier.de/ijleo

利用数字全息摄影技术在周期性和非周期性光学元件上进行改进和测量

Scratch enhancement and measurement in periodic and non-periodic optical elements using digital holography

Sonia Verma [a,b], Subhra S Sarma [a,c], Rakesh Dhar [b], Rajkumar [a,*]

[a] CSIR-Central Scientific Instruments Organization, Chandigarh 160030, India
[b] Department of Applied Physics, Guru Jambheshwar University of Science and Technology, Hisar 125005, Haryana, India
[c] Assam Don Bosco University, Guwahati 781017, Assam, India

ARTICLE INFO

Article history:
Received 16 July 2014
Accepted 3 August 2015

Keywords:
Digital holography
Scratch detection in optical elements
Optical inspection
Digital image processing

ABSTRACT

Scratch or flaw detection plays an important role in imaging optics and optical instrumentation. Even a minute scratch or crack can spoil coating and/or scatter incident light which causes irregularities/noise in the signal. Present paper describes use of digital holography for inspection of periodic and non-periodic optical elements for presence of any type of flaws like scratch, dust particles, irregularity etc. Digital image processing on numerically reconstructed wavefronts of the test samples provides enhanced image of the flaw. Various parameters of the flaws are measured. Experimental results of scratch on a glass plate and a lens and a thin hair on a grating and a mirror are presented.

1. Introduction

Optical elements are used in various instruments that play important role in many fields such as semiconductor industry, defense, space, astronomy, medical etc. For imaging applications optical surfaces should be precisely made, finished, handled and kept dust free [1]. Even a minute scratch, crack, irregularity in period or any other type of flaw in the optics will generate noise signal by scattering the incident light and thereby may severely affect the results. The scattered light can generate troublesome ghost interference patterns which may result in incorrect interpretation of the results [2]. Also in case of non-imaging fields, a scratch or dust particle can affect the desired results by generating noise signal. Thus, it is imperative to keep the optics scratch and dust free for obtaining accurate results. Various methods such as spatial filtering [3], Talbot and moiré methods [4,5], diffraction based method [6], interferometric, holographic and digital holographic methods [7–13] etc. are employed to detect these defects. Most of these methods are applicable only for the defect detection of periodic objects. It is necessity of time to develop such a technique which can be used for inspection of periodic structures such as semiconductor wafer or a grating as well as non-periodic components such as mirror, glass plate etc.

目前的工作描述了使用非轴菲勒全息摄影技术来检测周期性和非周期成分的缺陷。摘要采用互补金属氧化物半导体(CMOS)探测器对物体波前和参考波阵面进行了数字记录。在重建的波前，对每台计算机进行数字重建，并对其进行空间滤波。利用空间频率滤波，可以很容易地抑制像光栅和半导体晶片这样的周期性元件的周期性，因此只通过观察平面上的缺陷和缺陷的频率。对图像进行进一步的数字化处理后，会产生与缺陷和缺陷相关的增强信息，从而使它们的检测变得容易。同样地，对非周期物体的结构图像进行数字化处理，以有效地检测和测量这些元素的缺陷。本作品中使用的物品是玻璃板、镜子和光栅。

Present work describes use of off-axis Fresnel holography to detect flaws in periodic as well as non-periodic components. Interference of object wavefront and reference wavefront is recorded digitally using a Complementary metal oxide semiconductor (CMOS) detector. Reconstruction is performed numerically in personal computer and spatial filtering is performed digitally on the reconstructed wavefront. Using spatial frequency filtering one can easily suppress periodicity of periodic components like grating and semiconductor wafers thereby passing frequencies related only to defects/flaws in the observation plane. Further digital post processing of the image results in enhanced information related to defects and flaws making their detection easy. Similarly reconstructed images of non-periodic objects are also digitally processed for efficient detection and measurement of defects present on these elements. Objects used in this work are glass plate, mirror and grating.

2. Theory

1948年Dennis Gabor发现的全息摄影，是一种不使用成像光学的成像对象。它记录了测试对象的完整波前，并提供了与对象14的振幅和相位分布有关的全部信息。在数字全息摄影技术中，全息图是数字化的，在一台个人电脑上，用数字方法重建全息图。目前，在非轴几何中工作数字全息术被用来记录电子兴趣的对象，[illegible]

Holography, discovered by Dennis Gabor in 1948, is a process for imaging objects without using imaging optics. It records complete wavefront of the test object and provides whole information related to amplitude and phase distribution of the object [14]. In digital holography a hologram is recorded digitally and wavefront from recorded hologram is reconstructed by using numerical methods on a personal computer [15,16]. In present work digital holography in off-axis geometry is used to record the object of interest electronically and reconstruction is performed

光学元件在半导体工业、国防、航天、天文、医学等许多领域都发挥着重要作用。对于成像应用，光学表面应该精确地制造、完成、处理和保持灰尘1。即使是一分钟的划痕、裂缝、不规则或任何其他类型的缺陷，也会通过散射入射光产生噪声信号，从而可能严重影响结果。散射光会产生令人讨厌的鬼干涉模式，可能会导致结果2的不正确的内部变化。此外，在非成像领域，刮痕或尘粒可以通过产生噪声信号来影响所期望的结果。因此，为了获得准确的结果，保持光学划痕和灰尘free是必须的。各种各样的方法，如空间过滤3、Talbot和moir4,5、基于衍射的方法6、干涉测量、全息图和数字全息图7等，用来检测这些缺陷。这些方法大多只适用于周期性对象的缺陷检测。开发这种技术是需要时间的，它可以用来检查半导体晶片或光栅等非周期性元件，如镜、玻璃板等。

* Corresponding author. Tel.: +91 1722657811.
E-mail address: raj.csio@yahoo.com (Rajkumar).

http://dx.doi.org/10.1016/j.ijleo.2015.08.008
0030-4026/© 2015 Elsevier GmbH. All rights reserved.

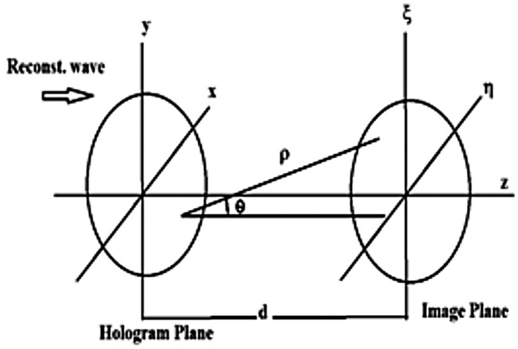

Fig. 1. Coordinate system.

在CMOS传感器的表面上叠加了一种被称为-ence的波和物体波。物体位于距离传感器的距离d处。在重建过程中，记录的全息图是用计算机生成的参考光束进行数字照明。这就导致了来自全息图的干涉条纹的入射光的衍射。这个衍射光形成了被记录物体的图像

numerically using Fresnel–Kirchhoff integral. A collimated reference wave and the object wave are superimposed at the surface of a CMOS sensor. Object is located at a distance d from the sensor. During reconstruction process, the recorded hologram is numerically illuminated with a computer generated reference beam. This results in diffraction of incident light from recorded interference fringes of the hologram. This diffracted light forms image of the recorded object.

Using Fresnel–Kirchhoff's approximation reconstructed field becomes [15]: 利用菲菲勒基尔霍夫的近似重建场

$$\Gamma(\xi,\eta)=\frac{i}{\lambda}\int\int_{-\infty}^{+\infty}h(x,y)R(x,y)\frac{\exp\left(-\left(2\pi/\lambda\right)\rho\right)}{\rho}\,dxdy \quad (1)$$

here (x,y) and (ξ,η) are coordinates of hologram plane and image plane, respectively, (as shown in Fig. 1) z is the direction of propagation; $h(x,y)$ = hologram function; $R(x,y)$ = reference plane wave; $\rho=\sqrt{(x-\xi)^2+(y-\eta)^2+(d)^2}$ is distance between a point in the hologram plane and a point in the image plane. Using Taylor series expansion around ρ

在这里(x,y)和(?)分别是全息平面和图像平面的坐标，(如图1所示)z是支柱-agation方向;h(x, y)=全息图像, R(x, y)=参考平面波;吗?? ?(x?)2?(y?)2?(d)2是在全息图平面上的一个点和图像平面上的一个点之间的距离。使用泰勒级数展开

$$\Gamma\left(\xi,\eta\right)=\frac{i}{\lambda d}\exp\left(-i\frac{2\pi}{\lambda}d\right)\exp\left(-i\frac{\pi}{\lambda d}\left(\xi^2+\eta^2\right)\right)$$

$$*\int\int_{-\infty}^{+\infty}h(x,y)R(x,y)\exp\left(-i\frac{\pi}{\lambda d}\left(x^2+y^2\right)\right)$$

$$\times\exp\left(i\frac{2\pi}{\lambda d}\left(x\xi+y\eta\right)\right)dxdy \quad (2)$$

Eq. (2) gives complex amplitude in image plane propagated from CMOS/hologram plane separated by distance d. This field is digitized by sampling the hologram function in hologram plane according to number of pixels and pixel size of CMOS and then converted into samples of image plane. The digitized field is stored in the computer in the form of a digital image which is further used for numerical reconstruction of the recorded object wavefront [17]. The intensity distribution corresponding to recorded hologram field is:

(2)在由距离d分离的cmo/全息平面上传播的图像平面的复杂振幅，通过在全息平面上的全息图，根据像素和象素的大小，然后转化为图像平面的样本，对全息图像进行数字化。数字化领域以数字图像的形式存储在计算机中，这一数字图像进一步用于数字重建的数字图像-前17。与记录全息图相对应的强度分布是

$$I\left(\xi,\eta\right)=\left|\Gamma\left(\xi,\eta\right)\right|^2 \quad (3)$$

The reconstruction process generates a bright patch corresponding to zero spatial frequency in the image known as un-diffracted zero-order term (or DC term). This DC term overlaps the desired reconstructed object image if minimum off-axis angle is not maintained during recording of interference pattern. So this term should be suppressed. To understand this, the intensity $I(x,y)$ of the optically generated interference pattern of reference beam $R(x,y)$ and $O(x,y)$ in hologram plane is given by coherent superposition of the

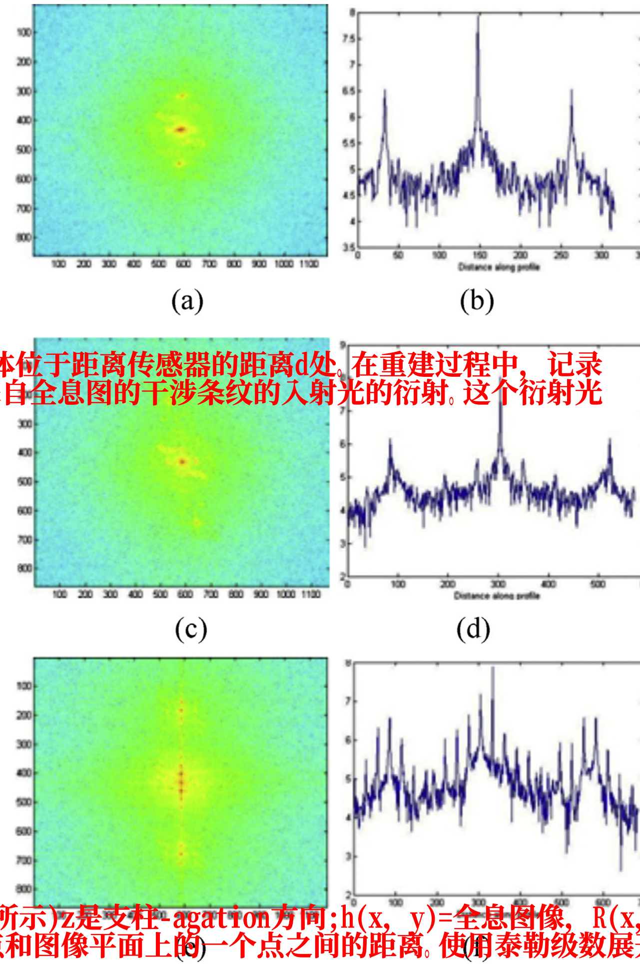

Fig. 2. (a) Fourier transform pattern of glass plate (c) of mirror and (e) of grating and (b), (d), (f) shows their respective intensity distributions.

two wave fields:

$$I(x,y)=\left|O(x,y)+R(x,y)\right|^2=R(x,y)^2+O(x,y)^2$$
$$+2O(x,y)R(x,y)\cos\left(\varphi_o-\varphi_R\right) \quad (4)$$

Here, first two terms lead to the DC term in the reconstruction process. Third term is varying between +2RO and −2RO from pixel to pixel in the CMOS. If first two terms are subtracted from total intensity, we will get the object term undisturbed by zero-term. Since, the average intensity of all pixels of the hologram matrix is

在这里，前两项是重建过程中的DC项。第三项是在CMOS中从像素到像素在+2RO到2RO之间变化。如果从总强度中减去前两个项，我们就会得到零项不受干扰的物体项。因为，全息图矩阵的所有像素的平均强度是

$$I_m=\frac{1}{N^2}\sum_{k=0}^{N-1}\sum_{l=0}^{N-1}I\left(k\Delta x,l\Delta y\right) \quad (5)$$

$R(x,y)^2+O(x,y)^2$ can be suppressed by subtracting this average intensity I_m from the hologram, giving: 可以通过从全息图中减去Im的平均强度来抑制

$$I'\left(k\Delta x,l\Delta y\right)=I\left(k\Delta x,l\Delta y\right)-I_m\left(k\Delta x,l\Delta y\right) \quad (6)$$

For $k=0\ldots N-1$; $l=0\ldots N-1$

The reconstruction of $I'\left(k\Delta x,l\Delta y\right)$ will result in an image which is free from zero order term. Here, Δx and Δy are the image pixel along x and y directions, respectively. It is also possible to filter the hologram matrix using high pass filter with low-cut-off frequency. For spatial filtering, Fourier transform is taken numerically of the recorded hologram, which generates three terms in Fourier plane (as shown in Fig. 2). The diffracted light having spatial frequency corresponding to object information will be focused at specific

重建过程产生了一个明亮的补丁，在被称为非衍射的零阶项(或直流项)的图像中，产生了零空间频率。该直流项与所期望的重建目标图像重叠，如果在干扰模式的记录中，最小的非轴角不是主要的。所以这一项应该被抑制。为了理解这一点，在全息图平面上，(x, y)和O(x, y)的求出干涉图样的强度I(x, y)是由两个波场的相干叠加所给出的。

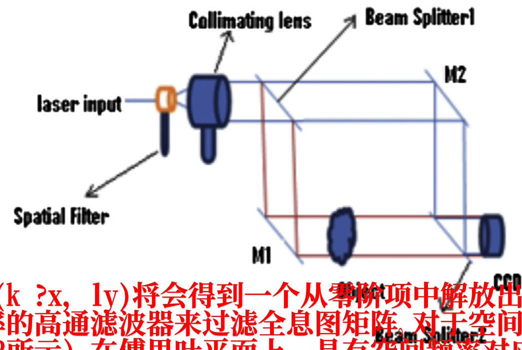

我的重建?(k ?x, ly)将会得到一个从零阶项中解放出来的图像。在这里，?x和?y分别是x和y方向上的图像像素。也可以使用低截止频率的高通滤波器来过滤全息图矩阵。对于空间滤波，傅里叶变换是用数字形式记录的全息图，在傅里叶平面上产生三项(如图2所示)。在傅里叶平面上，具有空间频率对应的空间频率的衍射光将聚焦在傅里叶平面上的特定点上。

Fig. 3. Holographic recording setup.

points in Fourier plane. These specific points of light are then filtered to get the useful information. Since, intensities of reference beam and object beam are almost equal, as a result diffraction efficiency of periodic pattern is much less as compared to the defect because the spatial frequency components of the defect term are much less than periodic spikes. After taking inverse transform reconstruction with conjugate reference beam provides enhanced defect out of original object. In case of non-periodic elements, the scattered intensity from defect is different from the object as well as of reference beam so its diffraction efficiency is different from rest of object part. Fig. 2(a, c and e) shows the Fourier transform patterns of glass plate, mirror and grating, respectively. These consists of three frequencies; the central frequency corresponds to DC term and other two are the ±1 diffraction terms. Fig. 2(b, d and f) shows their respective intensity distributions. By selecting accurate spatial frequency filter, other terms except corresponding to defect are suppressed so that defect term gets enhanced. After reconstruction a defect of 1.876 nm depth is found on the optical element.

这些特定的光点会被用来获取有用的信息。由于参考光束和目标束的强度几乎相等，因此，周期性模式的衍射效应与缺陷相比要小得多，因为缺陷项的空间频率分量比周期峰值要小得多。在进行逆变换后，用共轭参考梁进行重构，使原对象的缺陷得到增强。在非周期元素的情况下，由于缺陷的散射强度不同于物体和参考光束，因此其衍射效率不同于物体的其它部分。图2(a,c和e)分别显示玻璃板、镜子和光栅的傅里叶变换。这些由三个频率组成;中心频率对应于直流项而其他两个是1衍射项。图2(b,d和f)显示了它们各自的强度分布。通过选择精确的spa-频率滤波器，除与缺陷相对应的其他术语被抑制，从而使缺陷项得到增强。在重建后，在光学元件上发现了1.876纳米深度的缺陷。

Fig. 4. Block diagram of image processing techniques taken into account during defect detection.

3. Experimental details 实验细节

The experimental arrangement of holographic recording setup is schematically shown in Fig. 3. Here, scratch detection is performed through Fresnel digital holography with off axis holographic setup employing Mach-Zehnder geometry having four degrees of off-axis angle between reference and object wave. Light from laser source of wavelength 633 nm is expanded using spatial filter assembly. This spatially filtered beam is then passed through a collimating lens followed by a diaphragm of 9 mm diameter. The collimated beam is split into two beams using a variable beam splitter (beam splitter1). The object on which the defect is to be detected is placed in path of one of the beams now called as object beam. A CMOS camera (1024 × 1280) with pixel size of 6.7 μm is used to record the optically generated hologram. Various objects such as glass plate, mirror, lens and grating are used as test objects to detect their flaws. Recorded hologram is stored into a computer and is further processed numerically.

图3所示的全息记录装置的实验安排如图3所示。在这里，"划痕检测"是通过菲纳尔数字全息摄影技术来完成的，它采用了轴向全息图的方法，在参考和对象波之间，使用了马赫的几何图形，它有4度的偏离轴角。波长633纳米的激光光源使用空间滤光器组件进行扩展。这种空间过滤的光束经过一个平行光透镜，然后是一个9毫米直径的隔膜。用可变光束分裂-ter(光束分裂)，将平行光束分成两束。这个缺陷被检测到的物体被放置在一个被称为物体梁的光束的路径上。一个CMOS摄像头(1024 1280)，像素大小为6.7?m用于记录光学生成的全息图。玻璃板、镜子、透镜和光栅等各种物体都被当作检测对象来检测它们的缺陷。记录全息图存储在计算机中，并在数字上进行进一步的处理

In order to suppress DC light and to improve signal to noise ratio, average value of intensity is calculated numerically and then subtracted from total intensity of the hologram. Suppression of unwanted terms is achieved by high pass filtering. This pattern is further processed through Fresnel–Kirchhoff integral to get the reconstructed image. The image is processed through some layers of filters. First the image is threshold, which is needed for extraction of the desired image.

为了抑制直流光，提高信号的噪声比，用数值方法计算平均强度，然后从全息图的总强度中减去。对不想要的项的抑制是通过高通滤波实现的。这一模式通过菲勒尔-基尔霍夫积分得到进一步的处理，得到重建的图像。图像通过一些过滤层进行处理。首先，图像是阈值，这是提取所需图像所需要的。

Output image now consists of certain rough edges which are smoothened by dilation. A median filter is used to suppress noise from the reconstructed image. The image obtained now is further processed using 'diamond strel' so that we can get a smoothened and higher contrast images. These processes make the defect on test components clearly visible on the computer screen as shown in Figs. 5–8. All the processes are shown via block diagram in Fig. 4.

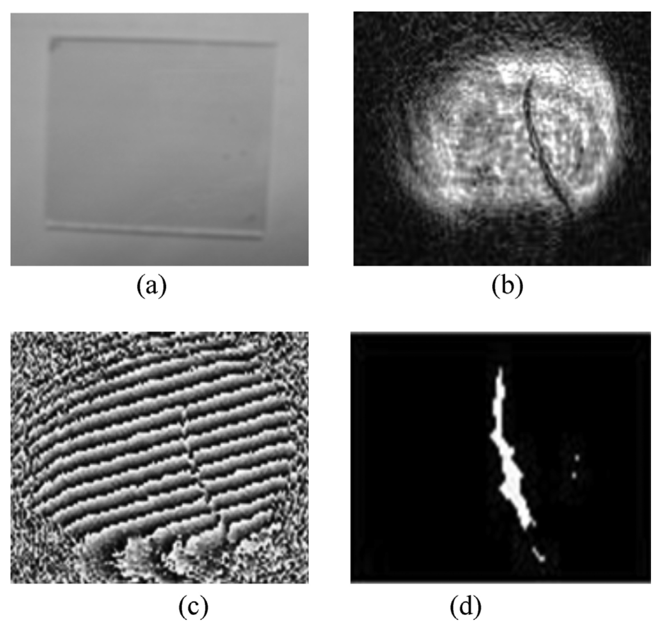

(a) (b) (c) (d)

Fig. 5. (a) shows the glass plate on which scratch is detected. Its reconstructed amplitude & phase. Patterns are shown in (b) and (c), respectively, and (d) shows filtered and enhanced image of scratch on glass plate.

(a)显示了被检测到的玻璃板。它重建的振幅和相位。模式显示在(b)和(c)中，并且(d)显示在玻璃板上经过过滤和增强的划痕图像

4. Result and discussion

Experiments are performed on a number of periodic and non-periodic optical components to test their flaws. These flaws are intentionally put on the test components. A scratch was developed on an optical glass plate (60 mm × 60 mm × 2 mm) as shown in Fig. 5(a) and its hologram was digitally recorded. After numerical processing the scratch is found to be 0.27 mm long and covering an area of 2.9 mm^2. The maximum and minimum width of this scratch is 0.05 mm and 0.0067 mm, respectively. The depth of the scratch

输出图像现在由一些粗糙的边缘组成，这些边缘被膨胀所平滑。中值滤波用于抑制重建图像中的噪声。现在得到的图像是用钻石链进一步处理的，这样我们就可以得到一个更光滑、更高对比度的图像。这些过程使测试组件的缺陷在计算机屏幕上清晰可见，如图5-8所示。所有的过程都通过图4中的块图来显示。

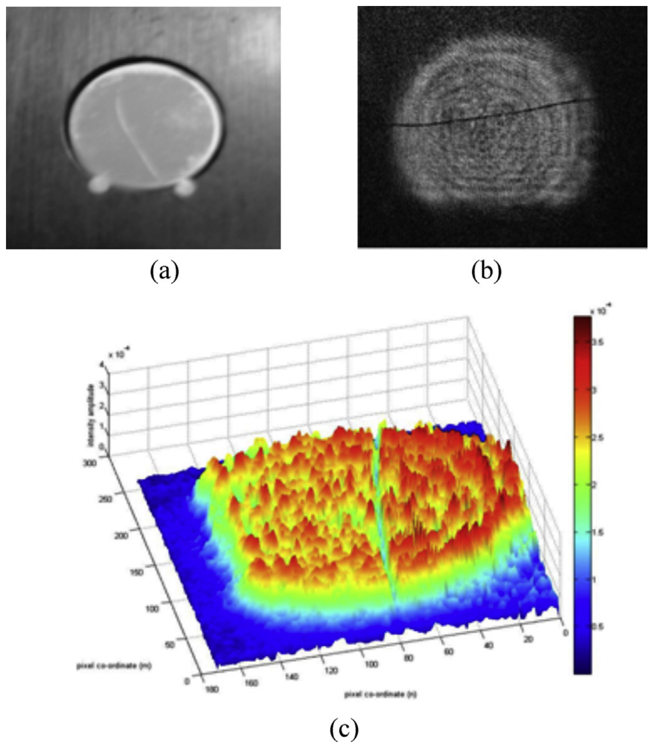

Fig. 6. (a) Human hair sample on mirror; (b) shows the reconstructed amplitude pattern of hair sample & (c) shows the side view of three dimensional amplitude distribution pattern of mirror with defect.

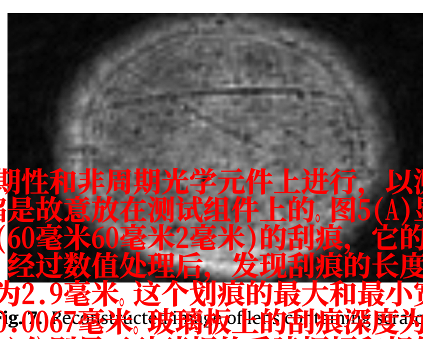

Fig. 7. Reconstructed image of lens containing scratch.

实验在许多周期性和非周期光学元件上进行，以测试它们的缺陷。这些缺陷是故意放在测试组件上的。图5(A)显示了一个光学玻璃板(60毫米60毫米2毫米)的刮痕，它的全息图是数字化记录的。经过数值处理后，发现刮痕的长度为0.27毫米，覆盖面积为2.9毫米。这个划痕的最大和最小宽度分别是0.05毫米和0.0067毫米。玻璃板上的刮痕深度为1.876纳米。图5(b)和(c)分别显示玻璃板的重建振幅和相位图像。

on glass plate is 1.876 nm. Fig. 5(b) and (c) shows reconstructed amplitude and phase images of glass plate, respectively.

Here it may be seen that the scratch on the plate is not visible with naked eye but it become visible in reconstructed images. Spatial filtering leaves scratch stands out clearly as now DC terms has been suppressed. Second experiment is performed on a mirror with a human hair kept on it as shown in Fig. 6(a). The reconstructed amplitude image is shown in Fig. 6(b) and (c) shows its 3D view in which x and y are the image co-ordinates in terms of number of pixels and z coordinate represents amplitude. The measured length of hair on mirror is 1.37 mm with a diameter of 20 μm. Here also the visibility of hair gets enhanced in reconstructed image as compared to seen by naked eye or a camera. A biconvex lens of focal length 4.35 cm at 633 nm wavelength is also tested using this method. During its testing, a converging beam from the test lens is allowed to interfere with the reference beam. The reconstructed image of test lens (Fig. 7) consists of two main scratches and numerically measured maximum length of scratch is 0.516 mm. The measured depth of the scratch is 1.34 nm.

在这里我们可以看到，盘子上的划痕并不是肉眼可见的，但在重建的图像中却可以看到。空间滤波留下的划痕很明显，因为现在DC项已经被抑制了。第二个实验是在镜子上进行的，上面有一个人的头发，如图6(a)所示。重建的振幅图像在图6(b)和(c)中显示了它的3D视图，其中x和y是图像坐标的图像坐标——图像和z坐标表示振幅。镜子上的头发长度为1.37毫米，直径为20米。与肉眼或相机相比，在重建的图像中，头发的可见度也得到了增强。采用这种方法，也可以对633纳米波长的焦度长度为4.35厘米的双onvex镜头进行测试。在测试过程中，测试透镜的一束会聚光束被允许干涉参考光束。测试镜头的重建图像(图7)由两个主要的刮痕和数值测量的最大长度为0.516毫米，测量的深度是1.34纳米。

A periodic optical element in the form of an optical grating having 6 lines/mm is also tested through this technique. Fig. 8(a) shows a hair sample on grating; (b) shows its reconstructed

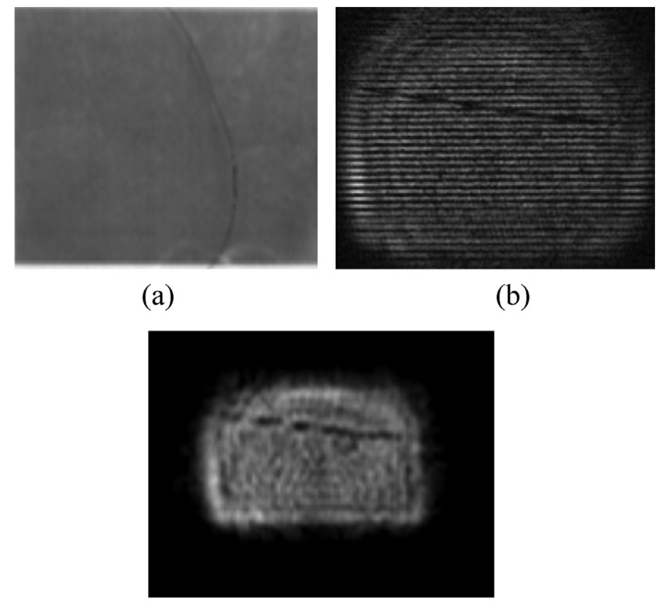

(a)光栅的头发样品；(b)重建光栅和(c)空间频率过滤重建的光栅图像。

Fig. 8. (a) Hair sample on grating; (b) Reconstructed hologram of grating & (c) Spatial frequency filtered reconstructed image of grating.

amplitude image. This image consists of both flaw as well as periodic pattern. To enhance the defect and to suppress periodic pattern spatial filtering is performed before reconstruction. Fig. 8(c) shows the spatial frequency filtered reconstructed image of grating. The measured length of flaw on grating is 1.62 mm and width 20.1 μm.

Here also spatial filtering of the reconstructed hologram enhances defect present in the periodic pattern. These results clearly show that digital holography can be effectively used for quality testing related to flaws and scratches of periodic as well as non-periodic optical components with high accuracy and fast speed.

在此同时，重建全息图的空间滤波增强了在周期模式中存在的缺陷。这些结果清楚地表明，数字全息摄影技术可以有效地用于质量检测，与周期和非周期光学元件的缺陷和划痕有关，而且精度高、速度快

5. Conclusion

Digital holography is a non-contact and mostly non-invasive method for recording and reconstruction of three-dimensional information of the test objects. It offers advantages of fast, parallel and dry processing, numerical analysis and compactness compared to other techniques. In present work, use of digital holography is demonstrated for inspection of optical elements for scratches and dust/foreign particles. The system is tested for detection and measurement of scratch on an optical glass plate and lens and dust/foreign particles on a mirror and grating. The spatial filtering is used to enhance the defect and a median filter is used to suppress the excess noise. Experimental result demonstrates applicability of this technique for inspection of periodic as well as non-periodic components and thus may prove useful in optical and semiconductor industry for quality testing of fabricated optical components and masks and/or circuits.

数字全息摄影是一种非接触式的非侵入性的方法，用于记录和重建测试对象的三维信息。与其它技术相比，它具有快速、并行和干燥处理、数值分析和紧实性等优点。在目前的工作中，利用数字全息摄影技术，对划痕和灰尘/异物的光学元件进行了检测。该系统的检测和测量是在光学玻璃板和镜片上，以及镜子和光栅上的灰尘/外来粒子的检测和测量。空间滤波用于增强缺陷，中值滤波用于抑制多余的噪声。实验结果表明，该方法对周期性和非周期成分的检测具有一定的适用性，因此在光学和半导体工业中，对光学器件、面具和/或电路的质量检测具有一定的应用价值

Acknowledgments

Authors are thankful to Dr. Bhargab Das, Mr. P. K. Baghel, Mr. R. C. Kalonia and Mr. D. P. Chhachhia for interesting discussions. The work is partially supported by Department of Science and Technology, New Delhi, India under Project No. GAP 316 and Council of Scientific and Industrial Research, New Delhi, India under OMEGA Project.

通过这种技术，一种具有6/毫米的光学光栅形式的周期性光学元件也被测试。图8(a)在光栅上显示一个头发样本；(b)显示其重建的振幅图像。这张图片既有缺陷也有周期性的图案。在重建前，要提高缺陷和抑制周期性的模式空间滤波。图8(c)显示了光栅的空间频率过滤重建图像。光栅上的缺陷长度为1.62毫米，宽度为20.1

References

[1] D. Malacara, Optical Shop Testing, third ed., John Wiley & Sons Inc, USA, 2007.
[2] H. Yang, G. Feng, J. Han, C. Wang, J. Su, Q. Xu, Q. Zhu, Scratches on optical component surface and its' modulation on injecting laser, High Power Laser Part. Beams 11 (2006) 1832–1836.
[3] E.U. Wagemann, H.-J. Tiziani, Spatial self-filtering using photorefractive and liquid crystals, J. Mod. Opt. 45 (1998) 1885–1897.
[4] E.U. Wagemann, T. Haist, H.-J. Tiziani, Defect enhancement using Fresnel imaging and a TN–LCD, Opt. Commun. 156 (1998) 231–234.
[5] E. Garbusi, J.A. Ferrari, Defect enhancement in periodic masks using 1/2-Talbot effect, Opt. Commun. 259 (2006) 55–59.
[6] B.J. Pernick, J. Kennedy, Optical method for fatigue crack detection, Appl. Opt. 19 (1980) 3224–3229.
[7] R. Kumar, S.K. Kaura, D. Mohan, A.K. Sharma, D.P. Chhachhia, A.K. Aggarwal, Defect inspection in photo-masks for integrated circuits using optical interferometers, Proc. Photonics (2006) 597 (University of Hyderabad, India).
[8] R.L. Fusek, L.H. Lin, Holographic optical processing for submicrometer defect detection, Opt. Eng. 24 (1985) 731–734.
[9] C. Uhrich, L. Hesselink, Submicrometer defect enhancement in periodic structures by using photorefractive holography, Opt. Lett. 17 (1992) 1087–1089.
[10] C. Uhrich, L. Hesselink, Submicrometer defect enhancement in periodic structures by using photorefractive holography: system design and performance, Appl. Opt. 33 (1994) 744–757.
[11] T. Okamoto, I. Yamaguchi, Real time enhancement of defects in periodic patterns by use of a bacteriorhodopsin film, Opt. Lett. 22 (1997) 337–339.
[12] C.E. Thomas Jr., et al., Direct to digital holography for semiconductor wafer defect detection and review, Proc. SPIE 4692 (2002) 180–194.
[13] M.A. Schulze, M.A. Hunt, E. Voelkl, J.D. Hickson, W. Usry, R.G. Smith, R. Bryant, C.E. Thomas Jr., Semiconductor wafer defect detection using digital holography, Proc. SPIE 5041 (2003) 183–193.
[14] P. Hariharan, Optical Holography: Principles, Techniques and Applications, Cambridge University Press, New York, 1996.
[15] U. Schnars, W.P.O. Jüptner, Digital Holography, Springer, Germany, 2005.
[16] U. Schnars, W.P.O. Jüptner, Digital recording and numerical reconstruction of holograms, Meas. Sci. Technol. 13 (2002) R85–R101.
[17] N. Verrier, M. Atlan, Off-axis digital hologram reconstruction: some practical considerations, Appl. Opt. 50 (2011) H136–H146.